Pramāṇa, Vol. 14, No. 4, April 1980, pp. 271–287. © Printed in India.

Imploding shocks in laser-driven fusion

S V LAWANDE, M R GUNYE and S V G MENON
Theoretical Reactor Physics Section, Bhabha Atomic Research Centre, Trombay, Bombay 400 085, India

MS received 3 October 1979; revised 22 February 1980

Abstract. The role of a sequence of imploding spherical and cylindrical shocks is investigated in the context of laser-driven fusion in deuterium-tritium pellets. An approximate analytical treatment of a convergent sequence of shocks is presented within the framework of gas-dynamic equations for self-similar motion. These analytical solutions are compared with the exact numerical solutions. The solutions display an explicit dependence on the relative strength between the successive shocks and the ratio of the final to the initial pressure in the shocks. These solutions are employed to estimate the fusion yield for a given input shock energy.

Keywords. Imploding shocks; gas dynamics; self-similar motion; laser-driven fusion.

1. Introduction

There is a considerable interest, in recent years, in the possibility of achieving fusion by irradiating DT pellets with intense pulsed laser beams (Nuckolls *et al* 1972; Brueckner and Jorna 1974). The central issue in laser-driven fusion is the compression and the subsequent non-uniform heating of the pellet which, in turn, involves the dynamics of the shocks driven by the pressures generated at the ablating surface. This problem can be investigated in the framework of gas-dynamic equations for self-similar motion (Zeldovich and Raizer 1967). The implosion by a single shock in an ideal gas was first studied by Guderley (1942). The approach of Guderley was subsequently employed by Somon *et al* (1962) and Goldman (1973) for analysing the behaviour of an imploding shock in a plasma simulated by an ideal gas with specific heat ratio $\gamma = 5/3$. The numerical results of Goldman (1973) have been employed by Brueckner and Jorna (1974) to estimate the fusion yield for an input shock energy in a DT plasma. Their analysis indicates clearly that the pellet compression required to achieve an appreciable fusion yield is certainly not possible with a single spherical shock.

A possible method of achieving high degree of compression is to launch successive shock waves from the ablating pellet surface. By tailoring the incident laser pulse suitably, one can produce a sequence of shocks of increasing strength such that the successive shocks do not overtake each other before coalescing near the centre of the pellet. The individual shocks should preferably be weak in order to minimise the initial heating of the pellet. The compression process following the passage of the first shock is then nearly adiabatic until all the shocks arrive simultaneously at the point of convergence. This leads to the formation of a coalesced shock moving inwards causing further compression and heating of the plasma near the centre of the

pellet. After reflection from the centre, the coalesced shock causes a sudden rise in the density and temperature of the plasma. Thus in a small region around the centre of the pellet, the density and temperature become sufficiently high so as to trigger thermonuclear reactions. The fast particles produced in these reactions may also contribute to further heating if their ranges are comparable to the radius of this central region. Thus the reflected shock initiates a thermonuclear burn wave propagating outwards at a supersonic speed.

The problem of compression by a convergent sequence of plane shocks has been treated by Brueckner and Jorna (1974). By an extension of this approach, approximate analytical solutions in spherical and cylindrical geometrics have been recently obtained (Jha and Chavda 1977; Chavda 1977; Chavda and Jha 1978). There are, however, some inherent drawbacks in the approximate analytical solutions (Jha and Chavda 1977; Chavda and Jha 1978) leading to a substantial deviation from the exact numerical results. The major discrepancy seems to arise from an erroneous determination of the position s^* of the reflected shock-front. Our motivation in this paper is three-fold: First, we suggest a correct procedure to obtain the value of s^* and the approximate analytical solutions. Secondly, we give exact numerical solutions displaying their dependence on the relative strength δ between successive shocks and the ratio χ of the pressures between the final and initial shocks. Thirdly, we employ these exact numerical solutions to relate the input shock energy required for a given fusion yield with the parameters δ and χ of the convergent sequence of shocks.

A mathematical formulation of the problem and the derivation of an approximate analytical solution is presented in § 2. The numerical scheme to obtain exact solutions is outlined in § 3. § 4 deals with the estimates for the fusion and shock energies. The discussion of the results obtained is given in § 5 and our conclusions in § 6.

2. Approximate analytical solutions

Brueckner and Jorna (1974) showed that a sequence of N non-overtaking shocks acts effectively as a single strong shock after the point of collapse. At this point where the shocks coalesce, the fluid variables are given by

$$p_N = p_0 (1+\delta)^N, \tag{1}$$

$$\rho_N = \rho_0 (p_N/p_0)^{\mu} \equiv \rho_0 \chi^{\mu}, \tag{2}$$

$$u_N = -C_0 \frac{\delta}{\gamma(x-1)} \left(1+\delta \frac{\gamma+1}{2\gamma}\right)^{-1/2} (x^{\nu}-1). \tag{3}$$

Here ρ_0, p_0 and C_0 are respectively the initial density, pressure and sound-speed of the fluid. The final density, pressure and fluid velocity are denoted by ρ_N, p_N and u_N respectively. This analysis simulates a DT plasma by an ideal gas with specific heat ratio $\gamma = 5/3$. The parameters δ and χ represent the rise in pressure between successive shocks and the ratio of the pressures between the final and initial shocks respectively. Finally, x, ν and μ are defined as

$$x = (1+\delta)^{1/2}\left(1+\delta\frac{\gamma-1}{2\gamma}\right)^{1/2}\left(1+\delta\frac{\gamma+1}{2\gamma}\right)^{-1/2}, \tag{4}$$

$$\nu = \ln x/\ln(1+\delta), \tag{5}$$

$$\mu = 1-2\nu. \tag{6}$$

The velocity U_N of the coalesced shock-front is given by

$$U_N = u_N - C_N(1+\delta)^{-1/2}\left(1+\delta\frac{\gamma-1}{2\gamma}\right)^{1/2}, \tag{7}$$

where the sound-speed C_N is

$$C_N = C_0\,\chi^{\nu}. \tag{8}$$

It may be pointed out that for the case of weak shocks ($\delta \ll 1$), $\mu \simeq 1/\gamma$ and $\nu \simeq (\gamma-1)/2\gamma$, leading to nearly adiabatic compression.

The subsequent motion of the fluid, after the shocks coalesce, is assumed (Jha and Chavda 1977) to be self-similar. The basic equations of such a self-similar motion can be cast in the form (Zeldovich and Raizer 1967):

$$d\ln Z/dV = (\gamma-1)/(\alpha-V) + \frac{(\eta\gamma-\eta+2)V-2}{\alpha-V}\frac{d\ln\xi}{dV}, \tag{9}$$

$$d\ln\xi/dV = \frac{(\alpha-V)^2-Z}{Z\eta(V-V_\infty)-V(1-V)(\alpha-V)} \equiv \frac{\mathscr{N}(V,Z)}{\mathscr{D}(V,Z)}, \tag{10}$$

$$d\ln G/dV = \frac{1}{\alpha-V} + \frac{\eta V}{\alpha-V}\frac{d\ln\xi}{dV}, \tag{11}$$

where the reduced fluid variables V, Z and G and the self-similarity variable and exponent α have their usual meaning (Zeldovich and Raizer 1967). The variable η assumes the values 1, 2 and 3 for the plane, cylindrical and spherical geometrics respectively, and

$$V_\infty = 2(1-\alpha)/\eta\gamma. \tag{12}$$

Equations (9)–(11) are to be solved with the initial conditions

$$Z(1) = (\alpha\, C_N/U_N)^2, \tag{13}$$

$$V(1) = \alpha\, u_N/U_N, \tag{14}$$

$$G(1) = \chi^{\mu}, \tag{15}$$

obtained from equations (1) to (3), (7) and (8). Equations (9) and (10) are sufficient to determine V and Z as functions of the self-similarity variable ξ and are of our main

concern in the subsequent discussion. Once V and Z are known as functions of ξ, G can be determined from the 'adiabatic integral' connecting all the three variables V, Z and G with ξ:

$$G = K\,\xi^{2\eta\lambda}\,(\alpha-V)^{2(1-\alpha)\lambda}\,Z^{\eta\alpha\lambda}, \tag{16}$$

where $\lambda = [(\eta\gamma-\eta+2)\,\alpha-2]^{-1}$

and the constant K is given by

$$K = G(1)\,[\alpha-V(1)]^{-2(1-\alpha)\lambda}\,[Z(1)]^{-\eta\alpha\lambda}.$$

In order that the solutions of (9) and (10) be physically meaningful, they must be single-valued functions of the variable ξ. This implies that $d\ln\xi/dV$ should not vanish in the interval $1\leqslant\xi<\infty$. From (10), it is clear that the numerator $N(V, Z)$ vanishes on the parabola $Z=(\alpha-V)^2$ and hence for non-zero value of $d\ln\xi/dV$, the denominator $\mathscr{D}(V, Z)$ must also vanish. This defines a singular point lying on the parabola through which the solution curve $Z=Z(V)$ must pass. This condition determines the self-similarity exponent α. The coordinates (V_s, Z_s) of this singular point are given by

$$V_s = \{\beta+[\beta^2-8\,(\eta-1)\,\gamma\alpha\,(1-\alpha)]^{1/2}\}/[2\,(\eta-1)\,\gamma], \tag{17}$$

$$Z_s = (\alpha-V_s)^2, \tag{18}$$

where $\beta = (\eta\alpha-1)\,\gamma + 2\,(1-\alpha)$.

Since V_s has to be real, one has

$$\beta^2 - 8\,(\eta-1)\,\gamma\alpha\,(1-\alpha) \geqslant 0,$$

or equivalently,

$$[\eta\gamma^2+4\gamma\,(\eta-2)+4]\,\alpha^2 - 2\,[\eta\gamma^2+2\gamma\,(\eta-3)+4]\,\alpha+(2-\gamma)^2 \geqslant 0. \tag{19}$$

An approximate value of α can be obtained by taking the equality sign in (19) and solving the quadratic equation. Of the two roots, the larger one α_0 is quite close to the actual value of α to be determined. It may be mentioned that in the case of $\gamma=5/3$, α_0 is 0·6869 and 0·8145 for the spherical and cylindrical geometries respectively. These approximate values of α are very close to those reported by Fujimoto and Mishkin (1978) recently. One may thus use the value α_0 to obtain approximate analytical solution. However, in order to obtain a more accurate solution, one needs to determine α with a better precision than α_0. This can be achieved by taking recourse to an iterative procedure discussed later in § 3. It may be mentioned here that for a sequence of weak shocks ($\delta \ll 1$), the initial point lies on the parabola $Z=(\alpha-V)^2$. In this special case, α is known analytically (Jha and Chavda 1977) and no iterative procedure is necessary.

The solution curve $Z=Z(V)$ is to be obtained in the three regions:

$$B(1 \leqslant \xi < \infty),\ C(\infty > \xi \geqslant \xi^*) \text{ and } D(\xi^* \geqslant \xi \geqslant 0).$$

The region B corresponds to that part traversed by the incident coalesced shock-front while the region C, characterised by the negative values of V, represents the part covered by the reflected shock. At $\xi=\xi^*$, reflected shock reaches the observation point and consequently, one applies the jump conditions

$$V_D = V_C + \frac{2(\alpha-V_C)^2-Z_C}{(\gamma+1)\,(\alpha-V_C)},$$

$$Z_D = \left(\frac{\gamma-1}{\gamma+1}\right)^2\left[1+\frac{2\,Z_C}{(\gamma-1)\,(\alpha-V_C)^2}\right]\left[\frac{2\gamma}{\gamma-1}(\alpha-V_C)^2-Z_C\right], \tag{20}$$

$$G_D = \left(\frac{\alpha-V_C}{\alpha-V_D}\right)G_C,$$

to connect the variables in region C to those in region D. It should, however be emphasised that the point ξ^* is neither known *a priori* nor can be determined correctly from the prescription of Chavda and Jha (1978). This will be shown explicitly by comparing their approximate values of ξ^* with those obtained from the exact numerical method due to Guderley (1942). To determine ξ^* correctly, one generates a curve $Z=Z_{D'}(V)$ using the jump conditions of (20) for every point on the curve $Z=Z_C(V)$ in region C. The curve $Z=Z_{D'}(V)$ intersects the solution curve $Z=Z_D(V)$ in region D at the point $\xi=\xi^*$ (Guderley 1942). Based on this procedure, an alternative equation to determine ξ^* will be presented subsequently.

It could be easily seen that the solutions of (9) and (10) can be written in the form

$$Z = Z'\,V^2\,(1-V)^{\eta(\gamma-1)}\,(\alpha-V)^{1-\gamma} \tag{21}$$

$$\xi = (\pm 1)^\alpha\,\xi'\,V^{-\alpha}\,(1-V)^{\alpha-1}. \tag{22}$$

The multiplicative phase factor $(\pm 1)^\alpha$ in (22) arises from the definition (Guderley 1942) of the self-similarity variable ξ in regions B and C respectively. The new variables Z' and ξ' are, in general, functions of V satisfying the equations,

$$d\ln Z'/dV = f_1(V)\,f_2(Z',\,V), \tag{23}$$

$$d\ln \xi'/dV = f_2(Z',\,V), \tag{24}$$

with $$f_1(V) = [\eta\gamma-\eta+2)\,V-2]/(\alpha-V),$$

$$f_2(Z',\,V) = \frac{Z'\,[\eta(\alpha-V)\,(V-V_\infty)-V(1-V)]}{Z'\,\eta V(1-V)\,(V-V_\infty)-(1-V)^{2+\eta-\eta\gamma}\,(\alpha-V)^\gamma}.$$

It should be noted that for small values of $|V|$ in regions B and C, the variables Z' and ξ' are nearly constant. Hence one can expand,

$$Z' = \sum_{n=0}^{\infty} a_n^B [V-V(1)]^n, \tag{25}$$

$$\xi' = \sum_{n=0}^{\infty} b_n^B [V-V(1)]^n, \tag{26}$$

in region B. It is clear that the constants a_0^B and b_0^B are determined from the initial conditions of (13) to (15). The other constants in (25) and (26) can be obtained by substituting these expansions in (23) and (24). However, in region C characterised by the negative values of $V, f_2(Z', V)$ becomes singular for certain values of V and Z'. It is, therefore, desirable to choose Z' as an independent variable and rewrite (23) and (24) as

$$dV/dZ' = (Z' f_1 f_2)^{-1}, \tag{27}$$

$$d \ln \xi'/dZ' = (Z' f_1)^{-1}. \tag{28}$$

The expansions appropriate in this region C are,

$$V = \sum_{n=1}^{\infty} a_n^C (Z'-Z_0')^n, \tag{29}$$

$$\xi' = \sum_{n=0}^{\infty} b_n^C (Z'-Z_0')^n, \tag{30}$$

where Z_0' and b_0^C are given by

$$Z_0' = \sum_{n=0}^{\infty} a_n^B [-V(1)]^n, \tag{31}$$

$$b_0^C = \sum_{n=0}^{\infty} b_n^B [-V(1)]^n. \tag{32}$$

The coefficients a_n^C and b_n^C with $n \geqslant 1$ can be obtained by substituting the expansions of (29) and (30) in (27) and (28).

To arrive at the solutions in region D, one has to impose (Guderley 1942) the boundary condition at $\xi = 0$. The appropriate variables to be used in this region are,

$$X = Z^{-1/2}, \qquad Y = VZ^{-1/2}. \tag{33}$$

It should be noted that both X and Y tend to zero as $\xi \to 0$ even though V remains finite. Employing these variables X and Y, equations (9) and (10) can be rewritten as

$$dY/dX = (Y/X) - F_1 [2(Y-\alpha X)/XF_2], \tag{34}$$

$$d \ln \xi/dX = 2(Y-\alpha X) [1-(Y-\alpha X)^2]/XF_2 \tag{35}$$

where $$F_1 = \eta(Y - X\,V_\infty) - Y(Y-X)\,(Y-\alpha X),$$

$$F_2 = 2(Y-\alpha X) - \eta X\,V_\infty - (Y-\alpha X)\,F_3, \tag{36}$$

$$F_3 = 2\alpha X^2 + [3-\gamma+\eta\,(\gamma-1)]\;Y^2 - [3-\gamma+\eta\,(\gamma-1)\,\alpha+2\alpha]\;XY.$$

It is clear that (34) is of the form

$$dY/dX = f(Y/X,\, X). \tag{37}$$

The general solution of this equation is given by Murphy (1960):

$$Y = \sum_{n=1}^{\infty} a_n^D\, X^n + \lambda\, X^\nu\, g(X), \tag{38}$$

where $g(X)$ is an analytic function of X, ν is the constant term in the coefficient of Y/X in (37) (ν should not be a positive integer) and λ is an arbitrary constant. If $\nu < 0$, the initial condition $Y=0$ at $X=0$ can only be satisfied by putting $\lambda=0$. If $\nu > 0$, the solution in (38) satisfies the initial condition $Y=0$ at $X=0$ for arbitrary value of λ, thus making the solution non-unique. For the present problem, it can be easily seen that

$$\nu = -\,[4\alpha^2(\eta - 1) + 2\alpha\eta V_\infty(\eta - 2) + \eta^2 V_\infty^2](2\alpha + \eta V_\infty)^{-2},$$

which is negative for the cylindrical ($\eta=2$) and spherical ($\eta=3$) geometries of interest. Hence, for the present problem, a unique solution

$$Y = \sum_{n=1}^{\infty} a_n^D\, X^n, \tag{39}$$

is obtained by determining the constants a_n^D by substituting (39) in the differential equation (34). Thus,

$$a_1^D = \alpha \text{ or } a_1^D = V_\infty,$$

$$a_2^D = 0,$$

$$a_3^D = V_\infty(\alpha - V_\infty)^2\,(1 - V_\infty([\eta\alpha + 2(\alpha - V_\infty)]^{-1}, \tag{40}$$

etc. The value $a_1^D = \alpha$ is, however, not acceptable in view of the fact that it violates the boundary condition $Z \to \infty$ as $\xi \to 0$. Using this solution in (39) and integrating (35), one obtains,

$$\ln \xi = b + b_0^D \ln X + \sum_{n=1}^{\infty} b_n^D\, X^n, \tag{41}$$

where b is a constant to be determined from the knowledge of the value ξ^* and

$$b_0^D = 2(\alpha - V_\infty)\,[2(\alpha - V_\infty) + \eta V_\infty]^{-1},$$

$$b_1^D = -\tfrac{1}{2}\,\eta V_\infty a_3^D\,(b_0^D)^2\,(\alpha - V_\infty)^{-2},$$

etc. Thus, in principle, the solutions of (9) and (10) are obtained in all the three regions, B, C and D. The solutions in the lowest order of approximation are given by

$$Z \simeq a_0^B\, V^2\,(1-V)\eta^{(\gamma-1)}\,(\alpha - V)^{1-\gamma}, \tag{42}$$

$$\xi \simeq (\pm 1)^\alpha\, b_0^B\, V^{-\alpha}\,(1-V)^{\alpha-1}, \tag{43}$$

in regions B and C. The $\pm$ sign in (43) refers to the regions B and C respectively.

$$Z \simeq a_3^B\,(V - V_\infty)^{-1}, \tag{44}$$

$$\xi \simeq b\, Z^{-b_0^D/2} \exp\,(b_1^D\, Z^{-1/2}), \tag{45}$$

in region D. It should be noted that the so-called analytical solutions in regions B and C given by equations (3.7) and (3.9) of Jha and Chavda (1977) are just the zeroth order approximations of (42) and (43). It may, however, be pointed out here that the solutions in region D given by equations (3.17) to (3.19) in the paper by Jha and Chavda (1977) are incorrect as can be seen from the comparison with our (44) and (45) which follow from a rigorous mathematical analysis. The solution in this region D has been subsequently discussed in another paper by Chavda and Jha (1978) wherein the correct dependence of Z on V is given. The constant C in equation (70) of Chavda and Jha (1978) is in agreement with our constant a_3^D in (40). However, our solution is obtained naturally from the initial conditions alone whereas the determination of C by Chavda and Jha (1978) requires the auxiliary constraint that the solution in this region D be of explosive type. It is clear from our analysis that no such auxiliary conditions are necessary for the solution in region D.

The parameter yet to be determined is the position ξ^* of the reflected coalesced shock-front. This can now be done with the help of solutions in regions C and D. Employing the solutions in (42) and (44) and the jump conditions in (20), one obtains the following transcendental equation for the value V_C in region C at the point $\xi = \xi^*$.

$$V_C - \alpha = \left(\frac{\gamma-1}{\gamma+1}\right)^2 \left(1 + \frac{2\omega_C}{\gamma-1}\right)\left(\frac{2\gamma}{\gamma-1} - \omega_C\right)\frac{(\alpha - V_C)^3}{(\gamma+1)\,a_3^D} \tag{46}$$

$$\times\,[(V_\infty - V_C)\,(\gamma+1) + 2\,(\alpha - V_C)\,(\omega_C - 1)],$$

where $\omega_C = Z_C\,(\alpha - V_C)^{-2}$,

Z_C being the value of Z in region C at $\xi=\xi^*$. The value ξ^* can thus be extracted from the expression for ξ in (43) by employing the value of V_C obtained by solving (46).

3. Numerical solutions

It is clear from the limiting behaviour of the variables Z and V, that the slope $d \ln \xi/dV \to \infty$ as $V \to 0$. Consequently equations (9) and (10) are not in a form suitable for numerical integration. It is, therefore, necessary to define the new variables Z' and ξ', introduced in equations (21) and (22). Equations (23) and (24) satisfied by these new variables can be used for numerical integration in region *B*. However, as discussed earlier in § 2, equations (27) and (28) have the appropriate form for numerical integration in region *C*. In region *D*, one has to use the variables X and Y in (33) and employ (34) for the numerical scheme. However, (35) cannot be integrated from the initial point $X=0$ since the slope $d \ln \xi/dX$ is indeterminate. The numerical integrations can be easily carried out by resorting to Runge-Kutta method.

The self-similarity exponent α is to be determined self-consistently. One starts with the initial guess value α_0 (§ 2) and the corresponding $V_{s0} = \beta/[2(\eta-1)\gamma]$. Integrating (9) from the initial value $V(1)$ to the value V_{s0}, yields the new value for Z_s which in turn yields the new value $V_s = \alpha_0 - \sqrt{Z_s}$. Substitution of this value in (17) determines the new value of α. This iterative scheme can be repeated till a desired accuracy is achieved. After the determination of α, the numerical solutions are obtained in regions *B*, *C* and *D*. One next generates the curve $Z=Z_{D'}(V)$ employing the jump conditions of (20) for every point on the curve $Z=Z_C(V)$. The curve $Z=Z_{D'}(V)$ represents the conditions that can be attained through shock waves after reflection at the origin. Since $Z=Z_{D'}(V)$ corresponds to the actual flow behind the reflected shock and at the same time contains the line $r=0$ (in the r–t diagram) as the trajectory of the particle, it follows (Guderley 1942) that the intersection of this curve with $Z=Z_{D'}(V)$ determines the exact position ξ^* of the reflected front. Once ξ^* is known (35) can be integrated from $X=X(\xi^*)$ to $X=0$ to obtain ξ as a function of V and Z in region *D*.

It may be mentioned here that for a sequence of weak shocks ($\delta \ll 1$), the self-similarity exponent α is analytically given by the expression

$$\alpha = (2\gamma^2+\gamma-1)/[\eta\gamma(\gamma-1) + \gamma^2+2\gamma-1]. \tag{47}$$

The numerical values of α for $\gamma=5/3$ in spherical and cylindrical geometries are 0·7368 and 0·8485 respectively.

4. Estimation of fusion yield

The numerical solutions thus obtained may be used to estimate the fusion energy E_f and the shock energy E_s. Following Brueckner and Jorna (1974), one gets, for spherical and cylindrical geometries,

$$E_f = 2^{\eta-3}\,\pi\, n_0^2\, W\, a^{-1}\, A^{-1/a} \times \int_0^{\infty} r^{\eta-1+1/a}\, dr \int_0^{\xi^*} \xi^{-1/a-1}\, G^2(\xi)\, \langle \sigma v \rangle\, d\xi, \tag{48}$$

where n_0 is the density of the DT-plasma, W is the energy released per fusion event and $\langle \sigma v \rangle$ is the Maxwellian averaged cross-section given by

$$\langle \sigma v \rangle = \sigma_0\, T^{-2/3} \exp(-B\, T^{-1/3}),$$
$$\sigma_0 = 19{\cdot}47 \times 10^{-8}\ \mathrm{cm^3\ sec^{-1}\ (^\circ K)^{2/3}}, \tag{49}$$
$$B = 4306\ (^\circ K)^{1/3}.$$

Using the saddle-point method to evaluate the relevant integral in (48), one obtains

$$E_f = [\eta^{\eta-4}\,\pi\, n_0^2\, W\, r_s^{\eta}\, t_s\, \langle \sigma v \rangle_s] \left[\frac{\eta}{2(1-\alpha)} (6\pi/\beta)^{1/2}\, I_1\right], \tag{50}$$

where $\langle \sigma v \rangle_s$ is the averaged cross-section evaluated at the saddle-point temperature T_s given by

$$T_s = (B/3\beta)^3,\ \beta = \frac{13 + \alpha\,(3\eta - 10)}{6\,(1-\alpha)}, \tag{51}$$

and

$$r_s = \left[A\ \xi^*\left(\frac{m\, Z(\xi^*)}{2\gamma\, k_B\, T_s}\right)^{\alpha/2}\right]^{1/(1-\alpha)},\quad t_s = (r_s/A)^{1/\alpha}, \tag{52}$$

$$I_1 = \int_0^{\xi^*} G^2(\xi)\ \xi^{-(1+1/\alpha)}\, d\xi. \tag{53}$$

The expression in the first bracket of (50) represents the fusion energy produced when a homogeneous DT-plasma of density n_0 is heated to a temperature T_s and confined for the hydrodynamic disassembly time t_s. The expression in the second bracket is the correction term due to shock compression.

The shock energy E_s can be expressed as

$$E_s = [(\eta+1)\,\pi\, r_s^{\eta}\, n_0\, k_B\, T_s] \left[\frac{2\gamma\, I_3}{\xi^{*\eta+2}\, Z(\xi^*)}\right], \tag{54}$$

where

$$I_3 = \int_0^{\xi^*} d\xi\ \xi^{\eta+1}\, G(\xi) \left[\frac{V^2}{2} + \frac{Z(\xi)}{\gamma(\gamma-1)}\right]. \tag{55}$$

The term in the first bracket of (54) represents the thermal energy of DT-plasma of density n_0 and temperature T_s. The correction due to the shock-compression and

heating is given by the term in the second bracket. It is convenient to express the shock energy as

$$E_s = C_\eta \, (E_f/E_s)^\eta \, (n_s/n_0)^{\eta-1} \, MJ, \tag{56}$$

where n_s is the density of the solid pellet and

$$C_\eta = \frac{\pi}{n^{\eta-1}} (\eta+1)^{\eta+1} \, \eta^{(3-\eta)\eta} \, (2\beta/3\pi)^{\eta/2} \left[\frac{2\gamma k_B \, T_s}{Z(\xi^*)}\right]^{(3\eta+2)/2}$$

$$\times \left[\frac{1-\alpha}{\sqrt{m} \, W \langle\sigma v\rangle_s}\right]^\eta \xi^{*\,[(\eta+1)\,(\eta+2)+\eta/\alpha]} \, I_3^{\eta+1} \, I_1^{-\eta}. \tag{57}$$

It is clear that (56) gives the scaling law relating to the input shock energy and the fusion energy. The coefficient C_η in (57) is a measure of the input energy required for break-even condition ($E_f=E_s$) in a solid DT pellet ($n_0=n_s$). As is evident from (53) and (55) the values of the integrals I_1 and I_3 depend on the compression factor G. It follows from the initial condition of (15) that the factor G scales as χ^μ where χ is the pressure ratio and μ is a function of the shock strength parameter δ. Thus the coefficient C_η varies as $\chi^{(1-\eta)\mu}$ and consequently it reduces considerably with increase in χ.

5. Results and discussion

The approximate analytical approach and the exact numerical scheme presented in §§ 2 and 3 respectively are employed to obtain the results are discussed here. We first discuss the case of multiple weak shocks for which the initial point A is on the parabola $Z=(\alpha-V)^2$ as pointed out earlier in § 3. The accuracy of the present analytical approximation can be seen from the plot of the reduced compression factor

$$\bar{G} = [(\gamma+1)/(\gamma-1)]\chi^{-1/\gamma} \, G$$

where G is the actual compression ratio ρ/ρ_0 against the reduced time $|s|=\xi^{-1/\alpha}$ in figures 1 and 2 for the spherical and cylindrical sequence of shocks respectively. The results of the exact numerical calculations and the approximate analytical method of Chavda and Jha (1978) are also shown in figures 1 and 2 for comparison. It is clear from these figures that the present scheme, even in the lowest order of approximation used in the present calculations gives a fairly good agreement with the exact numerical method. It is also seen from figures 1 and 2 that the results of Chavda and Jha (1978) in the regions B and C characterised by $s < s^*$ (s^* of their paper) agree with the present results as expected. However, their results (Chavda and Jha 1978) deviate appreciably from our results, and consequently from the exact results in region D is due to their incorrect determination of s^*. The accuracy of this analytical scheme can also be adjudged from the calculated values of $s^*=\xi^{*-1/\alpha}$ in the two geometries. For the spherical case, the analytical value of s^* is 2·95 which compares

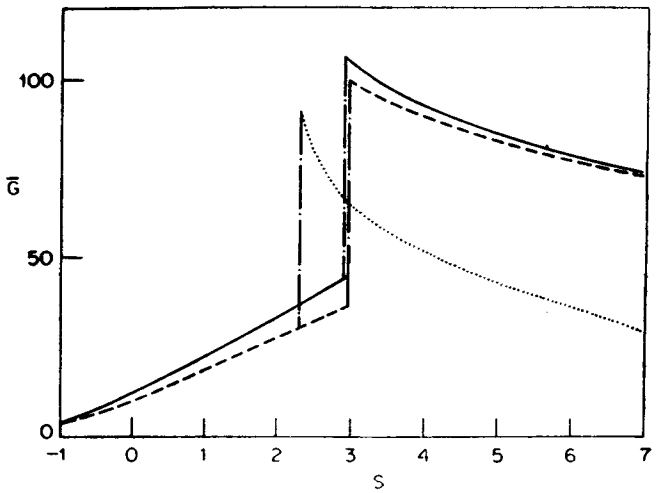

Figure 1. The reduced compression factor $\bar{G}$ is plotted as a function of the reduced time s for multiple spherical shocks. The solid and the dashed curves correspond to the exact numerical and an approximate analytical solutions respectively. The results of Chavda and Jha (1978) are shown by the dotted curve.

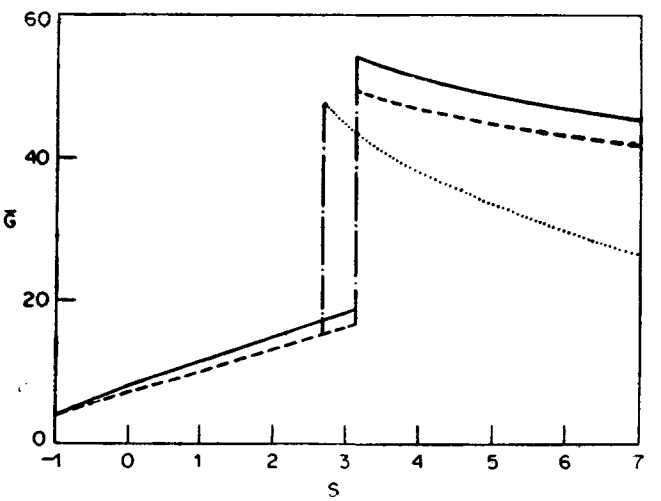

Figure 2. Same as figure 1 for cylindrical shocks.

very well with the value 2·91 obtained by the exact numerical scheme. For the cylindrical case, the analytical value of s^* is 3·10 which is very close to the exact value 3·12. It should be stressed here that the values 2·29 and 2·67 for the spherical and cylindrical cases obtained by Chavda and Jha (1978) are in considerable error. It is also worthwhile to mention here that even in the case of single spherical and cylindrical shocks our analytical approach yields s^* values 1·68 and 1·76 compared with the exact values 1·59 (Goldman 1973) and 1·69 (Somon *et al* 1962) respectively. On the other hand, the prescription of Chavda and Jha (1978) leads to the corresponding s^* values 2·17 and 2·45 which are also in substantial error.

In the framework of the numerical scheme presented in § 3, extensive calculations were performed for the convergent sequence of spherical and cylindrical shocks in a

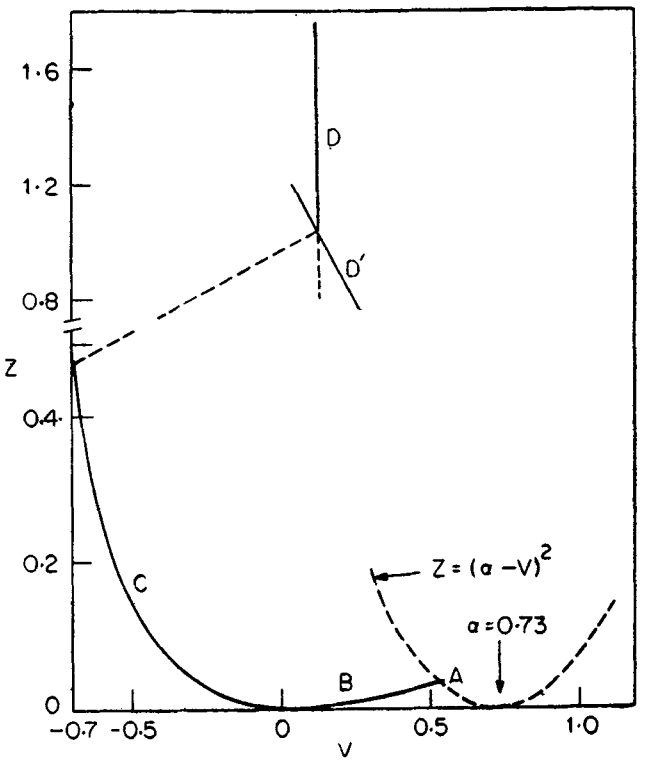

Figure 3. The integral curve $Z=Z(V)$ for the spherical case with $\delta=10^{-2}$ and $\chi=10^6$ is displayed. The initial point A, the singular point S, the origin O and the parabola $Z=(\alpha-V)^2$ are also shown.

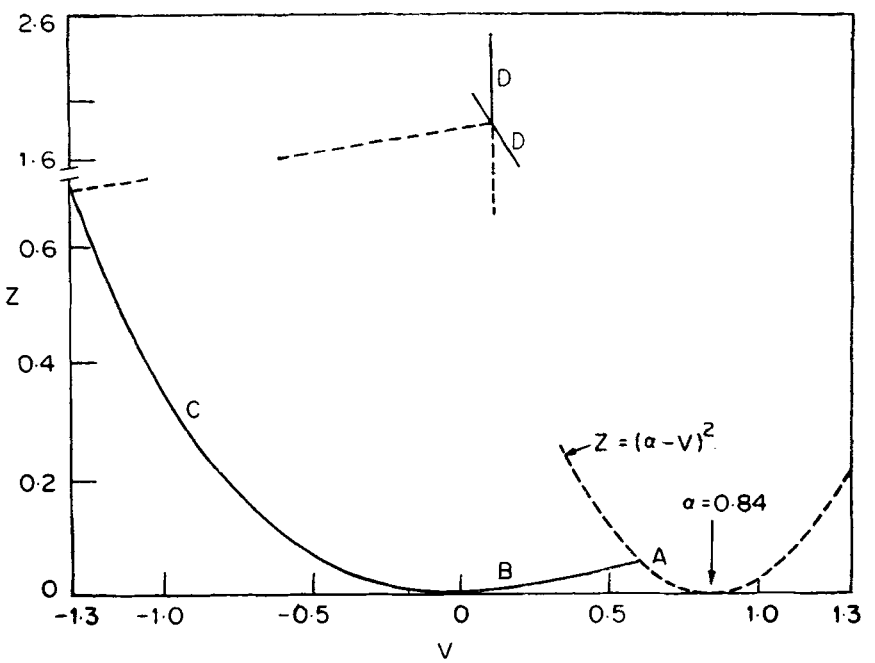

Figure 4. The cylindrical case with all other details as in figure 3.

DT plasma with various values for the shock-strength parameter δ and pressure-ratio χ. The integral curve $Z=Z(V)$ for a typical case with $\delta=10^{-2}$ and $\chi=10^6$ is displayed in figures 3 and 4 for spherical and cylindrical geometries respectively. In order to compare the compression achieved in the case of convergent sequential shocks to that of a single shock, we have plotted in figures 5 and 6 the reduced compression factor

$$\bar{G} = [(\gamma+1)/(\gamma-1)]\, \chi^{-\mu}\, G$$

against the reduced time s. The values of the parameters δ and χ chosen in figures 5 and 6 are the same as those employed in the calculation of the integral curves of figures 3 and 4. It should be mentioned here that the maximum compression achieved for a single strong shock in the case with $\gamma = 5/3$ is around 33 (Goldman 1973) and around 23 (Somon *et al* 1962) for spherical and cylindrical geometries respectively. However, the maximum values of the reduced compression factor $\bar{G}$ obtained in the present cases (figures 5 and 6) are about three times larger for the spherical case and about two times larger for the cylindrical case. Actual maximum compression G is, in fact, thousand times higher due to the scaling factor χ^{μ}. Figures 5 and 6 also display the variation of the reduced temperature $\bar{T}=Z/(\gamma\alpha^2 s^2)$ with the reduced time s. It is seen that, as compared to $\bar{G}$, $\bar{T}$ varies much slowly with s. It is also seen that the maximum value of $\bar{T}$ attained with a coalesced sequence of shocks is somewhat lower than that obtained in the case of a single shock (Brueckner and Jorna 1974). By comparing figures 5 and 6, one also observes that the reduced temperature $\bar{T}$ in the range $-1 \leqslant s < s^*$ is lower in the cylindrical case than in the spherical case; the

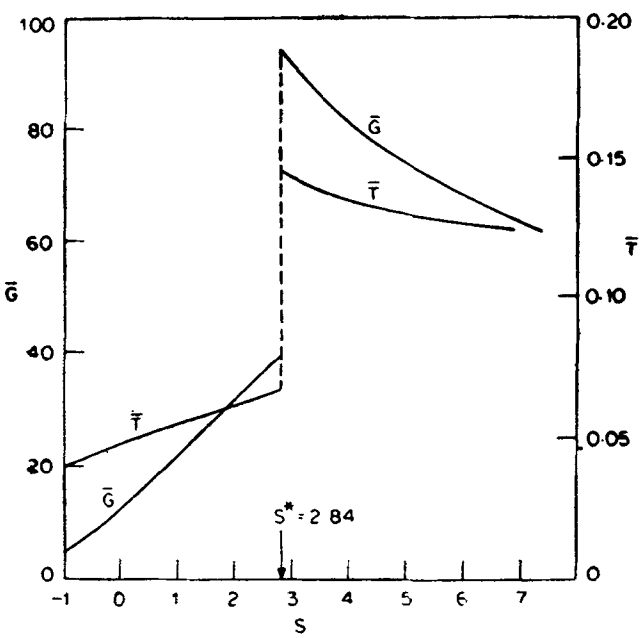

Figure 5. The reduced compression factor $\bar{G}$ and the reduced temperature $\bar{T}$ are shown as a function of the reduced time s for spherical geometry with $\delta=10^{-2}$ and $\chi=10^6$.

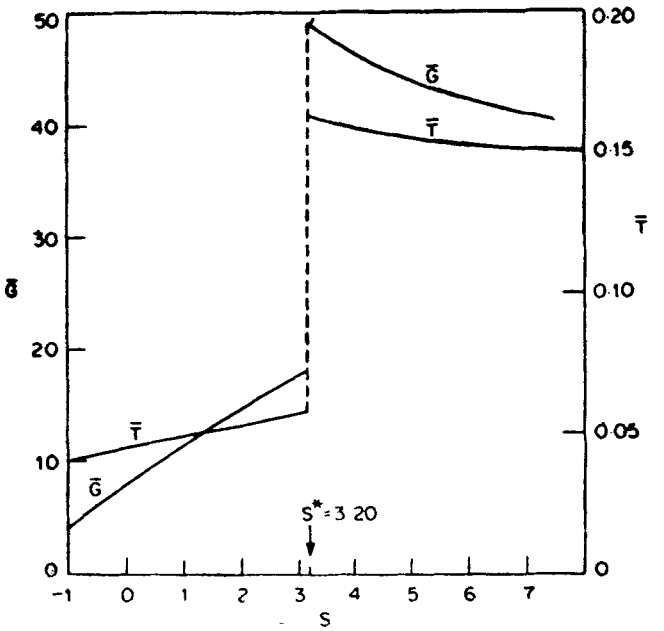

Figure 6. The cylindrical case with all other details as in figure 5.

situation is reverse in the range $s > s^*$. This behaviour, however, should not give the impression (Chavda and Jha 1978) that the cylindrical shocks are preferable to the spherical ones in the context of laser-driven fusion. The advantage in this behaviour of temperature $\bar{T}$ is offset by the compression factor $\bar{G}$ which is nearly a factor of two lower for the cylindrical case as compared with the spherical case. Moreover, the coefficient C_η discussed in § 4, varies as $\chi^{(1-\eta)\mu}$ and this indicates that for the cylindrical case ($\eta=2$), the input energy required for a given fusion yield is larger by a substantial factor χ^μ as compared to that for the spherical case ($\eta=3$). Thus a sequence of coalescing cylindrical shocks is less effective than the corresponding sequence of spherical shocks in achieving the desired implosion.

The detailed variation of the important parameters of the problem such as, the self-similarity exponent α, the discontinuity point s^*, the maximum value of the temperature $\bar{T}$, the compression factor $\bar{G}$ and the coefficient C_η with δ and χ for the spherical case is shown in table 1. It is clearly seen from table 1, that for a given value of χ, all these parameters are almost insensitive to the variation in δ. However, for a given δ, these parameters change significantly with χ. The reduced compression $\bar{G}$ increases significantly with increasing χ.

The exact solutions obtained for the convergent sequence of spherical shocks were employed to estimate the input shock energy required for a given fusion energy yield in a DT pellet plasma. As discussed in § 4, the relevant quantity to be evaluated here is the coefficient C_η in (50). It is seen from table 1 that the required input energy for a given fusion energy yield decreases rapidly with increase in the pressure ratio χ from a few megajoules to a fraction of a kilojoule. It is thus possible to reduce the required input energy drastically by using a coalesced sequence of weak shocks with a suitable pressure ratio in place of a single strong shock. This is, in

Table 1. The maximum values of the temperature $\bar{T}$, the compression $\bar{G}$ and the coefficient C_η along with other relevant quantities computed for a convergent sequence of spherical shocks in a DT plasma with $\gamma=5/3$ are displayed for various values of the shock strength δ and the pressure ratio χ.

δ	χ	a	s^*	$\bar{T}_{max}$	$\bar{G}_{max}$	C_η (*MJ*)
	10^2	0·7002	2·33	0·164	42·98	2·2
	10^3	0·7135	2·60	0·151	62·71	$4·2 \times 10^{-1}$
0·001	10^4	0·7222	2·73	0·147	77·67	$6·3 \times 10^{-2}$
	10^5	0·7277	2·80	0·145	87·75	$7·4 \times 10^{-3}$
	10^6	0·7311	2·84	0·144	94·61	$70· \times 10^{-4}$
	10^2	0·7001	2·33	0·164	43·06	2·2
	10^3	0·7135	2·60	0·151	62·83	$4·1 \times 10^{-1}$
0·01	10^4	0·7222	2·73	0·147	77·81	$6·2 \times 10^{-2}$
	10^5	0·7277	2·79	0·146	87·91	$7·3 \times 10^{-3}$
	10^6	0·7311	2·84	0·144	94·79	$6·7 \times 10^{-4}$
	10^2	0·7000	2·30	0·168	43·39	2·1
	10^3	0·7133	2·58	0·153	63·30	$3·9 \times 10^{-1}$
0·1	10^4	0·7219	2·71	0·149	78·08	$5·9 \times 10^{-2}$
	10^5	0·7274	2·79	0·147	88·89	$6·8 \times 10^{-3}$
	10^6	0·7308	2·82	0·146	95·57	$6·5 \times 10^{-4}$

fact, the major advantage of employing weak multiple shocks rather than a strong single shock.

6. Conclusions

The current interest in the laser-induced fusion has led us to the detailed investigations on the problem of compression and subsequent heating of a DT pellet. This problem essentially involves the dynamics of shocks driven by the pressures generated at the ablating pellet surface. Since a single strong shock is known to be rather inadequate to achieve the desired degree of compression, we have, in this paper, considered an alternative possibility of employing a coalesced sequence of spherical and cylindrical shocks. Approximate analytical solutions for this problem are presented and compared with the exact numerical solutions. It is found that even in the lowest order of approximation, our analytical results show a good agreement with the exact numerical results. The numerical solutions are employed to estimate the coefficient C_η which is a measure of the input shock energy required for a given fusion energy yield. It is found that the multiple shocks yield a very large compression as compared to that obtained with a single shock. The compression achieved is in fact strongly dependent on the pressure ratio χ and is almost insensitive to the strength parameter δ. The coefficient C_η scales as $\chi^{-2\mu}$ and $\chi^{-\mu}$ for the spherical and cylindrical shocks, thereby showing that the spherical shocks are much more efficient than cylindrical shocks in the context of laser-driven fusion.

References

Brueckner K A and Jorna S 1974 *Rev. Mod. Phys.* **46** 325
Chavda L K 1977 *Phys. Lett.* **A63** 316
Chavda L K and Jha S S 1978 *Pramāṇa* **10** 429
Fujimoto Y and Mishkin E A 1978 *Phys. Fluids* **21** 1933
Goldman E B 1973 *Plasma Phys.* **15** 289
Guderley G 1942 *Luftfahrt-Forsch.* **19** 302
Jha S S and Chavda L K 1977 *Phys. Rev.* **A15** 1289
Murphy G M 1960 *Ordinary differential equations and their solutions* (New York: van Nostrand)
Nuckolls J, Wood L, Thiessen A and Zimmermann G 1972 *Nature* (*London*) **239** 139
Somon J P, Linhart J G and Knoepfel H 1962 *Nucl. Fusion Suppl.* Part 2 717
Zeldovich Y B and Raizer Y P 1967 *Physics of shock waves and high temperature phenomena* (New York: Academic Press) Vol. 2, Ch. 12